Improved SPECT Using Simultaneous Emission and Transmission Tomography

Dale L. Bailey, Brian F. Hutton, and Paul J. Walker

Department of Nuclear Medicine, Royal Prince Alfred Hospital, and Department of Physics, NSW Institute of Technology, Sydney, Australia

A method is proposed to simultaneously record single photon emission and transmission tomographic (SPECT) studies to produce a map of attenuation coefficients (μ) for the body. A dual radionuclide SPECT acquisition is performed with a transmission source attached to a rotating gamma camera of lower energy than the emission radionuclide. Scatter from the emission source into the transmission window is removed by subtracting the predicted scatter distribution. The transmission image is then reconstructed to yield the map of attenuation coefficients for anatomic display or attenuation correction purposes. Experimental work has shown that the method can accurately derive μ values to ±2.5% in both phantom and patient studies, without increasing acquisition time. Preliminary attenuation correction experiments have demonstrated an accuracy of better than 5% for estimated activity.

J Nucl Med 28:844–851, 1987

Single photon emission computed tomography (SPECT) is widely used to study in vivo radiopharmaceutical distribution. Qualitatively, the modality gives excellent visualization of activity distribution, with improved contrast over conventional planar studies. Quantitative data from SPECT studies have been hampered for several reasons, mostly due to insufficient anatomic knowledge about the body in which the radiopharmaceutical is distributed. Accurate quantitation in SPECT requires, in particular, knowledge of the subject's contour and variation in attenuation coefficients (μ). It has been shown (*1*) that accurate attenuation correction is possible by combining an x-ray CT scan (for attenuation coefficients) with a SPECT study.

In this laboratory, a method of performing transmission tomography using a radionuclide flood source attached to a rotating gamma camera* was developed (*2*). The aim of that study was to measure effective μ values for attenuation correction of gated cardiac studies to calculate count-based left ventricular end-diastolic volume. This same technique can be applied to SPECT, with a transmission scan performed on each patient prior to the administration of radiopharmaceutical in order to attenuation correct the subsequent emission of SPECT scan. It is not desirable to perform separate transmission and emission studies because of the doubling of scan time, and the problem associated with repositioning and misalignment. The method described here performs both studies simultaneously using different radionuclides for the emission and transmission studies with separation by pulse height energy discrimination. This allows a method of concurrently recording structure (transmission) and function (emission) that has practical appeal.

MATERIALS AND METHODS

Data Acquisition

A PHA window of 20% is set over the photopeak of each radionuclide to collect a dual radionuclide study. The labeled tracer was deliberately chosen as the higher energy radionuclide, so that the conventional SPECT study remains unaffected by scatter using dual radionuclides.

The transmission radionuclide is contained in a flood tank, which is fixed to the gamma camera by a frame attached to the camera head, so that the patient is always located between the uncollimated transmission source and camera head as it rotates (Fig. 1). A low-energy, all-purpose collimator is fitted to the gamma camera. Images of transmission and radiopharmaceutical distribution are acquired at 64 angles for 20 sec per angle in a 64 × 64 word matrix.†

Received Apr. 30, 1986; revision accepted Nov. 3, 1986.

For reprints contact: D. L. Bailey, Department of Nuclear Medicine, Royal Prince Alfred Hospital, Camperdown NSW 2050 Australia.

Presented at the Annual Meeting of the Society of Nuclear Medicine, Washington, DC, June 1986.

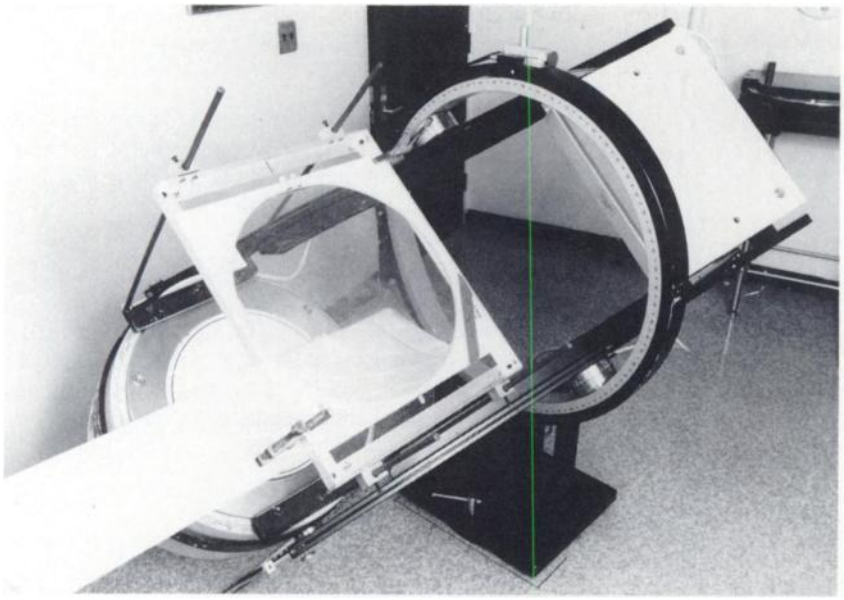

FIGURE 1
Tomographic camera with affixed transmission source.

Two sets of images result from this acquisition. The first is the usual emission scan as recorded in the upper photopeak energy window (g_u). The second contains the observed image (g_o) from the lower energy window, which contains the transmission scan degraded by scatter from the administered radiotracer. The major problem is to remove the scattered photon image of the upper energy radionuclide in the lower energy window (g_{ul}) from the observed image to leave the lower energy transmission image only (g_t).

Choice of Radionuclides

Any pair of radionuclides separable on sodium iodide (Tl) gamma spectroscopy are suitable for use with this technique. In this laboratory, ^{99m}Tc is being used as the emission nuclide and ^{153}Gd as the transmission source. ^{153}Gd has desirable properties of gamma emission at 98 and 103 keV, and a relatively long half-life ($t_{1/2}$ = 242 days) to give a semiper manent flood source. The radiation dose for a 30-min exposure to the transmission source is less than 100 gGy (10 mrad) for a source activity of 1.5 GBq (40 mCi).

Transmission Scan

In a transmission scan (free of any higher energy scattered photons) a measure is made at each angle of the number of photons transmitted to the detector head from the transmission source (the external flood tank) through the body. The recorded data are converted to attenuation coefficients by taking the natural logarithm of the ratio of unattenuated to attenuated counts, i.e.,

$$\frac{\ln\left[\frac{C_o}{C_x}\right]}{x} = \sum_i \mu_i, \qquad (1)$$

where x = the scaling factor in cm per pixel, C_o = unattenuated count rate of the transmission source, C_x = the transmission photon count rate, and $\sum_i \mu_i$ = the line integral of attenuation coefficients.

After performing this conversion it is possible to reconstruct, using conventional nuclear medicine tomographic software,‡ sections showing μ values and, hence, anatomy. It should be noted that because the flood source is uncollimated, the μ values measured are those appropriate for broad-beam geometric conditions. This is seen as an advantage because high statistics are attained as well as measuring the more relevant broad-beam μ value.

In the method proposed here, the transmission image contains scattered photons from the emission scan. These are removed by *predicting* the scatter image from the emission scan (g_u) and subtracting the result from the degraded lower energy image (g_o).

Scatter Prediction

Because two radionuclides are being used concurrently, the lower energy transmission images will contain scattered photons from the higher energy radionuclide, which need to be removed before transforming and reconstructing the attenuation sections. Each emission image is used to predict the scatter contribution into the lower window range. This is done by convolving the emission images with a predetermined scatter and subtracting this from the corresponding transmission plus scatter image. The convolution is done on the geometric mean (GM) of the opposed emission views.

It has been shown previously that the GM has many desirable properties for nuclear medicine studies (*3–7*). Geometric mean images have reasonably constant resolution with depth in an attenuating medium (*3,6*). Also, the number of photons detected from a point source at various depths does not vary greatly (*4, 6, 7*). It has been shown in this laboratory that the GM of the energy spectra of opposing views of sources at different depths are also relatively invariant (*6,8*). That is, there is a constant scatter ratio (k) of counts for any window of the energy spectrum to another, for a given radionuclide. Thus, the *number* of photons that can be expected to be scattered from a radionuclide's photopeak into a lower energy window can be estimated. The spatial *distribution* of the events scattered into the lower energy window must also be predicted.

Scatter Function

If the gamma camera is considered as a mathematically linear system (*9*), we may write for the GM images of the low energy window in a combined transmission/emission scan

$$g_o = g_t + f_u * h_{ul} \quad (2)$$

where g_o = observed image in lower window, g_t = transmission image, f_u = distribution of radiotracer, h_{ul} = the PSF for the upper energy radionuclide as seen in the lower energy (scatter) window, * indicates a convolution operation, and all functions are understood to be two-dimensional. In Fourier space this is

$$G_o = G_t + F_u \times H_{ul}, \quad (3)$$

where upper-case characters indicate the Fourier transform of their real space equivalents.

Scatter function(s) can be defined as that function which, when convolved with the upper energy image (g_u), yields a prediction of the scatter image observed in the lower energy window ($g_u * s$). The scatter function is determined by acquiring GM images of an upper energy point source (f_u) located at depth in an attenuating medium in the photopeak and scatter windows.

The two images may be represented as

$$g_u = f_u * h_u \quad \text{and} \quad g_{ul} = f_u * h_{ul}$$

for the photopeak and scatter windows respectively, where g_u = image of upper energy object in upper window, g_{ul} = image of upper energy object in lower window, f_u = upper energy radionuclide distribution, h_u = instrument PSF in upper window, h_{ul} = instrument PSF for the upper energy radionuclide in the lower energy window.

The scatter function(s) may be determined by deconvolving the PSF of a higher energy point source in its photopeak window (h_u) from the PSF of the same source as seen in the lower energy window (h_{ul}). That is,

$$S = \frac{H_{ul}}{H_u} \quad \text{(in Fourier space)}$$

There are difficulties with the Fourier method, however, because the smoothing required compromises the solution too greatly (*6*). Alternatively, the scatter function can be modeled mathematically. A suitable function is convolved with the photopeak window image (g_u) and the result compared with the observed lower window image (g_{ul}). The optimum scatter function is found by minimizing the sum of squared differences between the predicted image ($g_u * s$) and the true low-energy window image (g_{ul}). In this laboratory, a biexponential function has been used as a model of the scatter function. This approach has been shown to give an excellent estimate of scatter distribution independent of source depth (*6*).

As the scatter function(s) and the emission image (g_u) are known, it is possible to estimate the transmission component in the low energy window ($\hat{g}_t$) alone to be the observed lower window GM image minus the convolution of the upper energy GM image with the scatter function, appropriately scaled. That is,

$$\hat{g}_t = g_o - k(g_u * s)$$

where k is the predetermined scatter ratio from GM energy spectra of the radionuclide being used. This now provides separate images of transmission and emission.

Attenuation Correction

The attenuation coefficients are used for correction of the emission tomogram by calculating an attenuation correction factor for each voxel within the body. A first order correction can be applied (*1*) using the equation

$$C(x, y) = \left[\frac{1}{M}\sum_{i=1}^{M} \exp(-\mu l(x, y, \theta_i))\right]^{-1}$$

The correction factor for the point (x, y) is the inverse of the average of the attenuation factors for M projections over 360° about the point. Each point in the emission section is then multiplied by the corresponding correction factor.

EXPERIMENTAL WORK

Scatter Prediction

The scatter function was determined by taking GM images of point sources and vials containing ^{99m}Tc at depths of 5, 10, 15, 20, and 25 cm in a water tank with similar dimensions to a patient. This gave images in the upper photopeak (g_u) and lower (or scatter) photopeak (g_{ul}). The solution for the scatter function(s) was then found from these images. Subsquent to this, patient images in both windows have been collected and scatter functions determined to assess variations in the scatter function.

In a similar way, GM energy spectra were obtained to determine the scatter ratio (k). The spectra were collected on point sources of ^{99m}Tc measured at various depths in water from a gamma camera with a low-energy, all-purpose collimator attached, and collected on a multichannel analyzer.

Transmission Data

A number of questions arose when considering a transmission scan of a different radionuclide energy to the radiopharmaceutical for attenuation correction. First, the energy dependence of the attenuation coefficient was examined. Also, it was necessary to know if the coefficients measured are applicable under broad-beam geometric imaging conditions.

The energy dependence was studied by measuring the attenuation coefficient using a variety of materials for both ^{99m}Tc and ^{153}Gd. Using a point source, a number of attenuations (wood, paper, perspex, sawdust, water) were interspersed between the collimated gamma camera and the source and the attenuation coefficients calculated. This gave a measure of attenuation under planar imaging conditions. Transmission single photon computed tomographic studies using both ^{153}Gd and ^{99m}Tc flood sources were acquired on a composite attenuation phantom, to measure the attenuation coefficient expected in a tomographic study. The phantom covered a range of materials with densities (p) of 0.02–1.2 g·cm^{-3}. A similar study was conducted on a human volunteer, having both ^{153}Gd and ^{99m}Tc transmission scans performed. All data were acquired as for a SPECT study: 64 angles for 20 secs per angle.

To investigate the correlation between attenuation coefficients measued by transmission and emission, experiments were performed with attenuators to simulate each situation. A 10-cm thick perspex block was placed between the gamma camera face and a point source of ^{99m}Tc, to simulate the

transmission condition. For the emission situation a second block was placed behind the source. Measurements were made at various attenuator–gamma camera distances.

A qualitative comparison was made of the resolution of transmission data and emission data for tomography. For the emission case, a water-filled tank containing syringes of total volumes in the range 0.5–50 ml (7.6–33.4 mm diameter) was imaged. The syringes contained ^{99m}Tc with radioconcentration of 0.2 mCi·ml^{-1} (7 MBq·ml^{-1}). For the transmission case, the syringes were filled with nonradioactive water and the surrounding media in the tank was sawdust ($p = 0.2$ g·cm^{-3}). The geometry for both studies was identical.

Patient Studies

A small group of patients was studied to assess the technique. Geometric mean (anterior/posterior) transmission images were collected on a subject prior to the administration of radiopharmaceutical. This gave the transmission images alone (g_t). The subject was then studied after tracer administration and GM images were collected in both photopeak and scatter windows, with and without the transmission source present. Subsequent investigations were done to compare the μ values measured by transmission tomography before tracer administration compared with after administration, that is, from scatter corrected transmission tomography.

Attenuation Correction

Preliminary experiments were performed to determine total radioactivity in phantom studies. Attenuation correction was done by calculating the average attenuation to each point from the attenuation coefficient map. A chest phantom consisting of plastic flasks containing sawdust and ^{99m}Tc and surrounded by water was imaged. The same phantom, both with water instead of sawdust in the flasks, was also studied. The activities of ^{99m}Tc were in the range (1–2.3 mCi) (35–85 MBq) and the ^{153}Gd transmission source activity was 40 mCi. (1.5 GBq). These activities are representative of the values encountered in routine clinical situations.

RESULTS

Scatter Prediction

Detailed results pertaining to the determination of the scatter function and the scatter ratio are presented elsewhere (*6,9*). Briefly, the method is to synthesize a two-dimensional biexponential function. This function is then convolved with the upper peak image to produce a predicted scatter image, which is compared with the recorded lower peak true scatter image and the sum of squared deviations between the two images is calculated. The function that minimizes this difference is taken to most accurately model the true scatter function. The model of the scatter function(s) in use in this laboratory is a biexponential of the form

$$s(r, \theta) = Ae^{-br} + e^{-cr},$$

where r = radial distance in cm, and A, B, and c are constants. The values for the constants that gave a minimum for the sum of squared deviations determined on a series of phantoms and patients were: A = 18, b = 1.92 cm^{-1}, and c = 0.167 cm^{-1}.

TABLE 1
Comparison of True and Predicted Scatter Counts

Region	True counts	Predicted counts	Difference (%)
Lung	402	439	+8.4
Heart	608	603	−0.8
Stomach	421	403	−4.3

The scatter ratio (k) for use with ^{99m}Tc/^{153}Gd was determined from GM energy spectra of point sources at varying depths in a water tank and has been validated from GM images of phantoms and a group of patients having ^{99m}Tc studies, and has been found to be 0.60 ± 0.04. Table 1 shows a scatter prediction capability of better than 10% of the true scatter for a range of tissues including lung, liver, heart, and bone. This figure may be further improved by more accurate modeling of the scatter function.

Figure 2 shows the GM energy spectrum of ^{99m}Tc. The error bars indicate 1 s.d. of the values for all depth combinations at a number of points in the spectrum. This illustrates the depth independence of the GM spectrum, thus, allowing the number of photons scattered into the lower window to be predicted independent of source location.

Transmission Data

Figure 3 demonstrates the linear relationship for

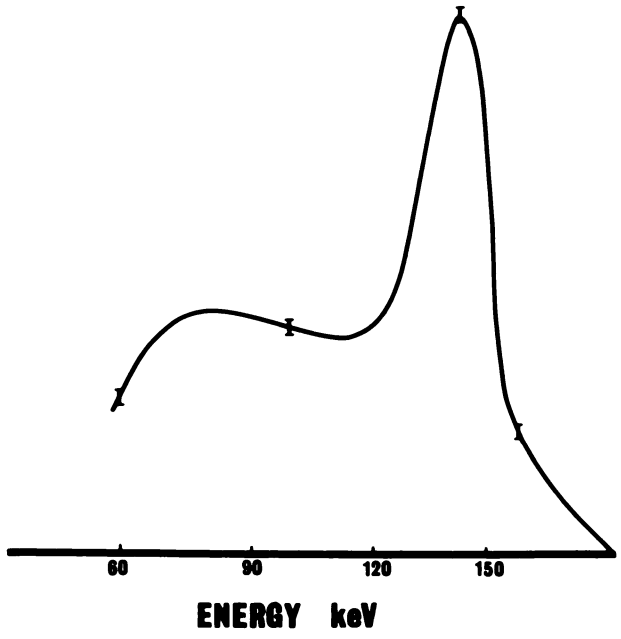

FIGURE 2
GM energy spectrum for ^{99m}Tc. The spectrum is the mean of the GM counts of a point source for different depth combinations from 5 to 25 cm in water.

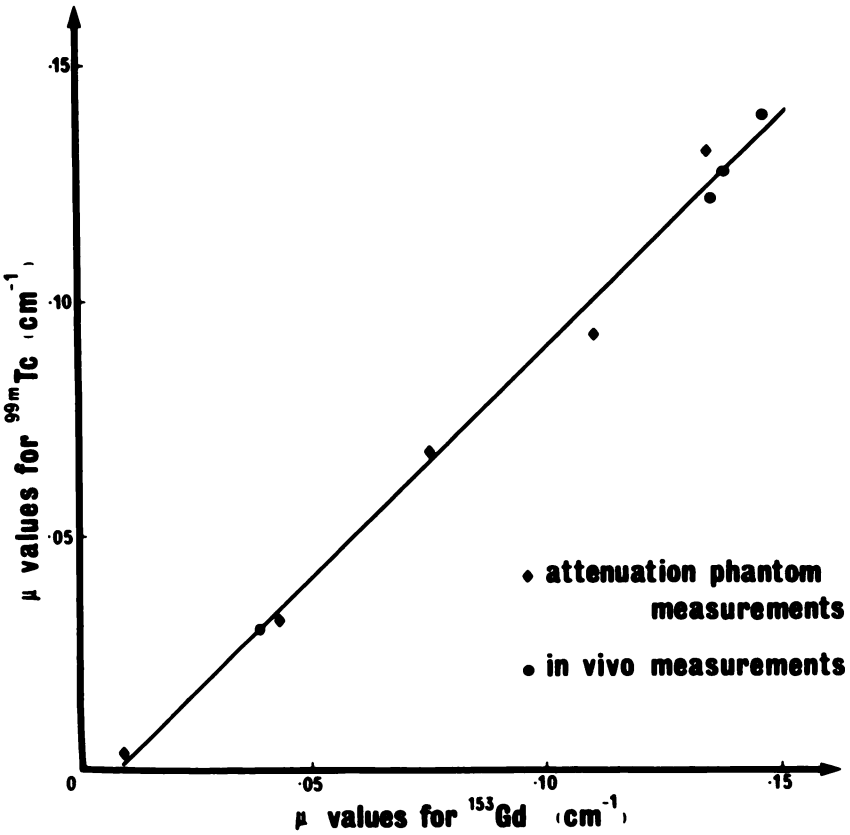

FIGURE 3
Broad-beam attenuation coefficients for ^{153}Gd and ^{99m}Tc ($\mu_{Tc} = 0.98\ \mu_{Gd} - 0.007\ cm^{-1}$; r = 0.998).

attenuation that was found to exist between the 98/103 keV gamma photons of ^{153}Gd and the 140 keV photons of ^{99m}Tc ($\mu_{Tc} = 0.98\ \mu_{Gd} - 0.007\ cm^{-1}$; r = 0.998). Data are shown in Table 2 for ^{99m}Tc and ^{153}Gd transmission scans on both the attenuation phantoms and on a volunteer. This confirmed similar findings using point sources of ^{153}Gd and ^{99m}Tc with different attenuators in conventional planar images on the gamma camera. Thus, the μ value for ^{99m}Tc can be determined from the ^{153}Gd μ values.

The propriety of using a transmission μ value for correcting an emission scan for the broad-beam geometric case was confirmed as the measured attenuation coefficient for transmission was shown to be equivalent to that measured by the emission source in a number of different attenuator geometries. This has been affirmed by at least one other group (*10*).

Resolution in the transmission study has been shown to be comparable with that of the emission study by scanning the previously described phantom. In both studies, the syringes measuring down to 12.5 mm in diameter were visualized.

TABLE 2
Measured Attenuation Coefficients for a Range of Materials for ^{153}Gd and ^{99m}Tc

Material	μ_{Gd} (cm^{-1})	μ_{Tc} (cm^{-1})
Phantoms		
Sawdust	0.010	0.004
Wood	0.043	0.034
Paper	0.075	0.068
Water	0.11	0.093
Perspex	0.129	0.120
In vivo		
Lung	0.039	0.030
Heart	0.135	0.122
Chest wall	0.138	0.128
Bone	0.146	0.140

Patient Studies

The images in Figure 4 are the GM of the anterior/posterior views of the thorax for a SPECT study of a patient with ^{99m}Tc-labeled RBC for (A) the emission, (B) true transmission, (C) true scatter, and (D) true scatter plus transmission. The image on the left in Figure 5 shows (A) the predicted scatter for this study, whereas, on the right is (B) the result of subtracting the predicted scatter from the observed lower window image. This should be compared with the true transmission image of Figure 4 (B).

Figure 6 shows the attenuation and emission images for two transverse sections through the thorax from a [^{99m}Tc]MAA perfusion lung dual emission/transmission study after scatter correction. Table 3 shows the attenuation coefficients measured by transmission tomography before tracer administration compared with after tracer administration on scatter corrected images

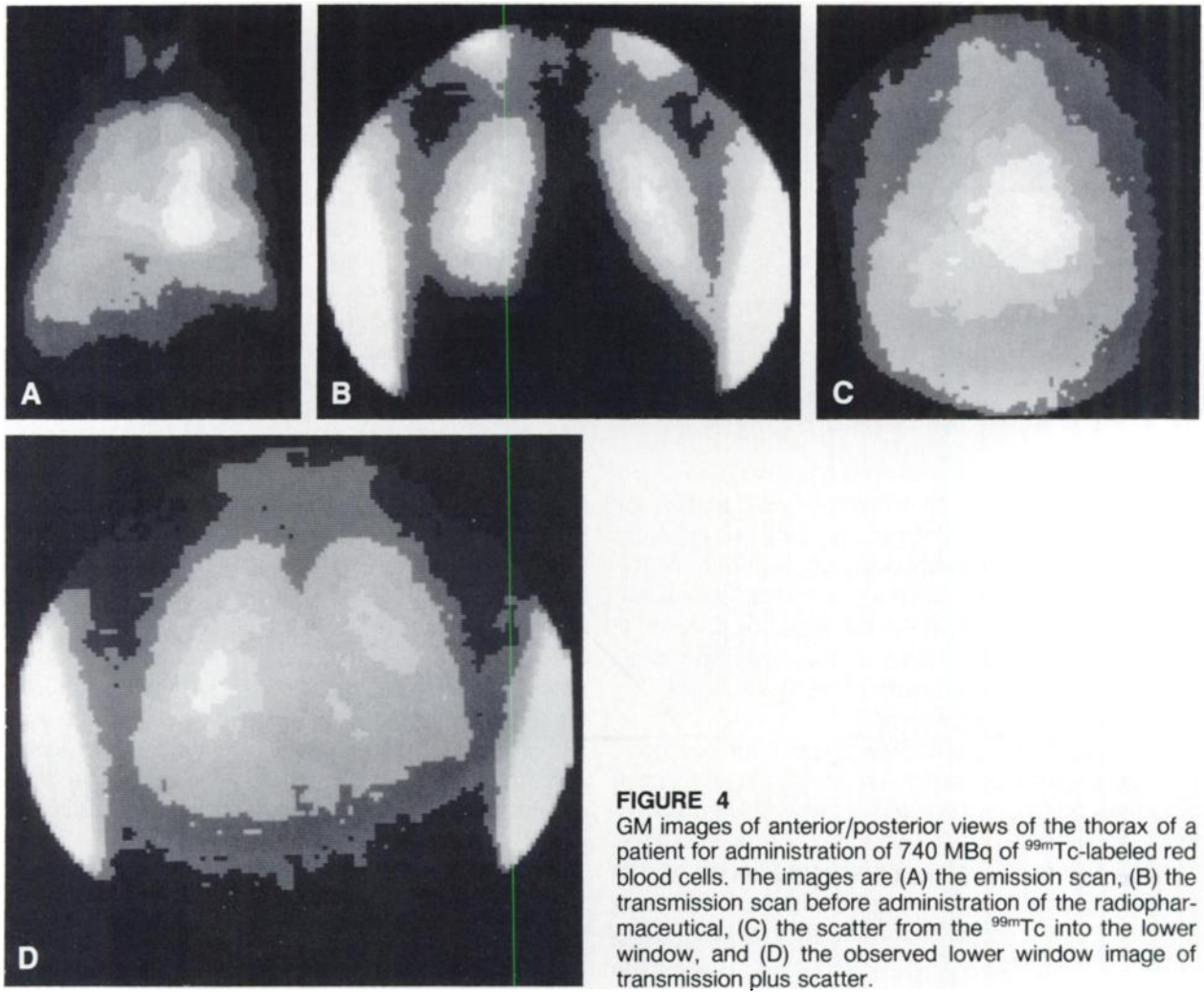

FIGURE 4
GM images of anterior/posterior views of the thorax of a patient for administration of 740 MBq of ^{99m}Tc-labeled red blood cells. The images are (A) the emission scan, (B) the transmission scan before administration of the radiopharmaceutical, (C) the scatter from the ^{99m}Tc into the lower window, and (D) the observed lower window image of transmission plus scatter.

from the dual emission/transmission study. The results were obtained using the previously stated values for the scatter function and scatter ratio.

Attenuation Correction

In the experiments to determine total radioactivity, attenuation correction maps of correction factors for each voxel were calculated. The total activity was calculated by multiplying the uncorrected transverse slice count for each voxel by the attenuation correction factor for the voxel and the camera/collimator sensitivity factor, i.e.,

$$\text{Activity (MBq)} = \frac{\text{Unattenuated emission count (cps)}}{\text{Camera sensitivity (cps}\cdot\text{MBq}^{-1})} \times \text{Attenuation correction factor}$$

When the correction factors were applied to the emission tomographic slices there was better than 5% agreement between estimated and measured ^{99m}Tc activities (Table 4). Further validation of these preliminary results is currently in progress. Quite clearly, the achievable accuracy will depend on the adequacy of the scatter function and the relative number of transmitted and scattered photons. Nevertheless, these initial results demonstrate the potential offered by the technique to provide accurate quantitation at no expense to study time.

TABLE 3
Attenuation Coefficients from True and Scatter Corrected Transmission Tomography

Region	True μ value (cm^{-1})	Scatter corrected μ value (cm^{-1})
Lung	0.030	0.028
Heart	0.122	0.119
Bone	0.135	0.132
Liver	0.127	0.128

TABLE 4
Results of Attenuation Correction Using Scatter Corrected Transmission Tomography

Flask	Calibrated activity MBq	Calibrated activity mCi	Measured activity MBq	Measured activity mCi	Difference (%)
Sawdust 1	77.9	2.11	76.5	2.07	−1.8
Sawdust 2	83.5	2.26	80.3	2.17	−3.8
Water 1	52.3	1.41	52.8	1.43	+1.0
Water 2	35.5	0.96	36.0	0.97	+1.4

DISCUSSION

The technique described offers potential in three main avenues for nuclear medicine SPECT studies: (a) the ability to accurately depict the patient's contour, independent of radiopharmaceutical distribution; (b) the display of subject anatomy as well as radiopharmaceutical distribution to aid interpretation of SPECT studies; and (c) the possibility to accurately determine μ values for each voxel within the field-of-view for attenuation correction purposes.

The need for an accurate body contour has been previously recognized as a severe problem in any direct or indirect attenuation correction protocol (*11*). This is most readily seen in studies of the head where body contour may vary significantly between slices (*12*).

Although SPECT displays are useful there is often a need to have a better appreciation of the anatomy present in the image. This is particularly true where radiopharmaceutical uptake is in an abnormal focus (such as tumor imaging) or is regional (as in perfusion imaging), rather than a whole organ. Because the technique uses simultaneous studies, registration and patient repositioning problems are eliminated and it is possible to show radiopharmaceutical distribution along side the corresponding anatomic (transmission) slice or, alternatively, to superimpose activity distribution on anatomy.

The ultimate aim of the technique is more accurate attenuation correction and, hence, better quantitation in SPECT using the attenuation coefficients measured in the patient, rather than assume a constant μ for all tissues. This is of particular importance in areas of the body where large differences in μ exist, such as the thorax. For this application quantitatively accurate scatter correction is necessary. The degree of error introduced by the dual radionuclide approach has not yet been fully assessed. Work is in progress to investigate the change in shape of the scatter function near a nonscattering medium such as the body edge, and the degree of difference in scatter function and ratio for different attenuating media. In this way it may be possible to determine individual scatter functions each for the head, chest, and abdomen. The approach currently being taken is to determine an average scatter function from a group of patients, using the least squares method described, for different regions of the body.

This technique offers three pieces of information for SPECT studies without in any way compromising the emission scan of radiopharmaceutical distribution. It is universally applicable using suitable radionuclide combinations, and the only new equipment required is a

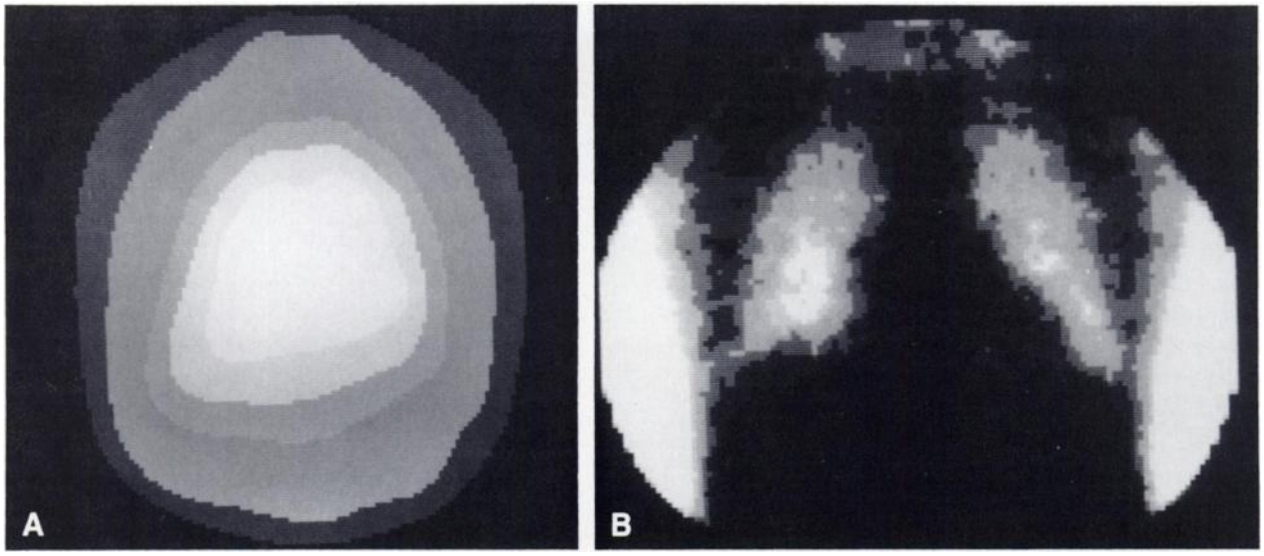

FIGURE 5
Results of scatter prediction. A: the scatter image predicted from the emission image, B: the results of subtracting the predicted scatter from the observed lower window image.

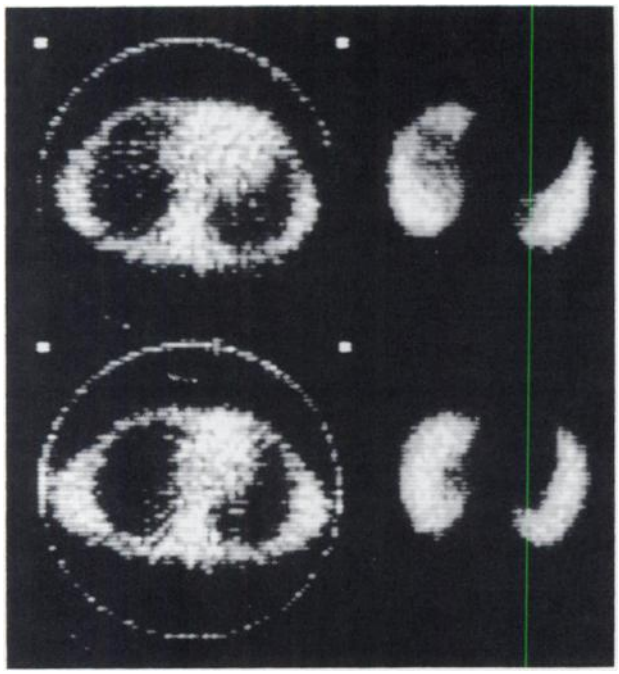

FIGURE 6
Corresponding attenuation and emission transverse tomographic sections from a dual radionuclide emission/transmission study of a patient for a lung perfusion scan. (The upper image is at the ventricular level and the bottom image is at the level of the atria.).

simple metal frame to attach the transmission source to the gamma camera. Further work is being pursued toward better attenuation correction protocols using this method.

NOTES

* IGE-400AT, General Electric Corporation Medical Systems, Milwaukee, WI.

† PDP-11/34, Digital Equipment Corporation, Marlboro, MA.

‡ SPETS-11, Nuclear Diagnostics.

REFERENCES

1. Moore SC. Attenuation compensation. In: Ell PJ, Holman BL, eds. Computed emission tomography, Oxford University Press, 1982:339–360.
2. Hutton BF, Fulton RR, Bailey DL, et al. Absolute cardiac chamber volume utilising a direct measure of attenuation from radioisotope transmission tomography. *ANZ J Med* 1984; 14:930.
3. Larsson SA. Gamma camera emission tomography. *Acta Radiol Suppl* 1980; 363: 17–32.
4. Tothill P, Galt JM. Quantitative profile scanning for the measurement of organ radioactivity. *Phys Med Biol* 1971; 16:625–634.
5. Axelsson B, Msaki P, Israelsson A. Subtraction of compton scattered photons in SPECT. *J Nucl Med* 1984; 25:490–494.
6. Hutton BF, Jayasinghe MAC, Bailey DL, et al. Artifact reduction in dual radionuclide subtraction studies. *Phys Med Biol* 1985; (submitted).
7. Fleming JS. A technique for the absolute measurement of activity using a gamma camera and computer. *Phys Med Biol* 1979; 24:176–180.
8. Jayasinghe MAC. Possible improvements for the subtraction imaging technique in radio-immuno detection of cancer [Thesis]. Sydney: University of NSW, 1984.
9. Beck RN, Zimmer LT, Charleston DB, et al. Advances in fundamental aspects of imaging systems and techniques. In: Medical radioisotope scintigraphy, Vol 1. Vienna: IAEA, 1973:3–45.
10. Macey DJ, Marshall R. Absolute quantification of radiotracer uptake in the lungs using a gamma camera. *J Nucl Med* 1984; 23:731–735.
11. Hawman EG. Impact of body contour data on quantitative SPECT imaging. In: Proceedings of the Third World Congress of Nuclear Medicine and Biology, 1982:1038–1041.
12. Herzog H, Weiler H, Vogt E, et al. Improved brain SPECT using a single head SPECT-camera with a conventional LFOV detector. *Eur J Nucl Med* 1985; 11:560.